

# PRELIMINARY REPORTS



## USE OF THERMAL IMAGERY FOR ESTIMATION OF CORE BODY TEMPERATURE DURING PRECOOLING, EXERTION, AND RECOVERY IN WILDLAND FIREFIGHTER PROTECTIVE CLOTHING

Thirimachos Bourlai, PhD, Riana R. Pryor, MS, Joe Suyama, MD, Steven E. Reis, MD, David Hostler, PhD

### ABSTRACT

**Background.** Monitoring core body temperature to identify heat stress in first responders and in individuals participating in mass gatherings (e.g., marathons) is difficult. **Objective.** This study utilized high-sensitivity thermal imaging technology to predict the core temperature of human subjects at a distance while performing simulated field operations wearing thermal protective garments. **Methods.** Six male subjects participating in a study of precooling prior to exertion in wildland firefighter thermal protective clothing had thermal images of the face captured with a high-resolution thermal imaging camera concomitant with measures of core and skin temperature before, during, and after treadmill exercise in a heated room. Correlations and measures of agreement between core temperature and thermal imaging-based temperature were performed. **Results.** The subjects walked

an average ( $\pm$  standard deviation) of 42.6 ( $\pm 5.9$ ) minutes and a distance of 4.2 ( $\pm 0.6$ ) km on the treadmill. Mean heart rate at the end of exercise was 152 ( $\pm 33$ ) bpm and core body temperature at the end of exercise was 38.3°C ( $\pm 0.7^\circ\text{C}$ ). A visual relationship and a strong correlation between core temperature and thermal imaging of the face were identified in all subjects, with the closest relationship and best agreement occurring during exercise. The Bland-Altman test of agreement during exercise revealed the majority of measurement pairs to be within two standard deviations of the measured temperature. **Conclusions.** High-resolution thermal imaging in the middle-wave infrared spectrum (3–5  $\mu\text{m}$ ) can be used to accurately estimate core body temperature during exertion in a hot room while participants are wearing wildland firefighting garments. Although this technology is promising, it must be refined. Using alternative measurement sites such as the skin over the carotid artery, using multiple measurement sites, or adding pulse detection may improve the estimation of body temperature by thermal imagery. **Key words:** heat stress; thermography; thermometry; performance; assessment

PREHOSPITAL EMERGENCY CARE 2012;16:390–399

### INTRODUCTION

Exertional heat stress is common in many occupational groups, including soldiers and firefighters.<sup>1–4</sup> Heat stress that is created while wearing protective equipment is termed *uncompensable heat stress* (UHS). UHS occurs from an inability of a person's body to dissipate heat when he or she is performing routine operations while wearing thermal protective clothing and other forms of personal protective equipment. Because of this increase risk of heat-related illness, early identification and mitigation of heat stress are critical for sustaining these types of operations. However, monitoring of core body temperature is difficult in the field. Measurement of core body temperature using rectal thermometers or ingestible capsules during

Received August 23, 2012, from the Lane Department of Computer Science and Electrical Engineering (TB), West Virginia University, Morgantown, West Virginia; and the Department of Emergency Medicine, Emergency Responder Human Performance Laboratory (RRP, JS, SER, DH), and the Department of Medicine, Division of Cardiology University of Pittsburgh (SER), Pittsburgh, Pennsylvania. Revision received January 6, 2012; accepted for publication January 7, 2012.

The authors thank the participants for their time and dedication to firefighter health and safety. They would also like to thank Ms. Jennifer Erin, MS, and Priya Khorana, MS, for their assistance with data collection. They would also like to thank FLIR Systems, Inc., for their technical support during this project.

No conflicts of interest, financial or otherwise, are declared by the authors.

Address correspondence and reprint requests to: David Hostler, PhD, University of Pittsburgh, Department of Emergency Medicine, 3600 Forbes Avenue, Suite 400A, Pittsburgh, PA 15261. e-mail: hostlerdp@upmc.edu

doi: 10.3109/10903127.2012.670689

routine operations is impractical, expensive, and difficult to integrate into daily operations.<sup>5,6</sup> Additionally, during large events (e.g., marathons) and other mass screening situations, it is too labor-intensive to position workers to deploy any type of direct temperature monitoring system for large numbers of individuals.

A true surrogate temperature assessment tool or technique that can accurately estimate the core temperature during exertion and at rest has been difficult to identify. Oral and axillary thermometers, temporal artery scanners, and skin temperature devices used in adults have poor correlation and accuracy in their ability to monitor core body temperature at rest and under exertional or uncompensable heat stress. One potential solution that may be a surrogate for real-time field monitoring of core body temperature is an imaging process that takes advantage of the cutaneous vasculature in human skin.

Superficial arteries are located immediately under facial skin. This superficial arterial distribution of the face branches from the external carotid artery shortly after leaving the aortic arch. The compliance of the artery during pulsatile flow results in capillary flow, diffusion effect, and tissue deformation followed by the convection of heat to the skin. As such, it may be possible to take advantage of the anatomy of the face and facial vasculature to estimate core body temperature using thermal imaging.

An improved approach of using standoff physiologic monitoring through passive (thermal) imaging to measure cardiac pulse was proposed by Bourlai et al.<sup>7,8</sup> In that work, a highly sensitive thermal imaging camera was used to monitor the blood vessels of human faces over time. The camera used was a lower-end model (lower spatial resolution) than the camera used in this study, both operating at the same spectral (thermal) band (middle-wave infrared, 3–5  $\mu\text{m}$ ). The advantage of middle-wave infrared cameras over cameras operating in the visible or active infrared (0.8–2.5  $\mu\text{m}$ ) bands is that they are capable of detecting the heat radiation of human skin. In addition, middle-wave infrared cameras can be set to detect heat radiation every 1/30 second while achieving high thermal sensitivity (i.e., close to 0.01°C). Another advantage of thermal middle-wave infrared imaging is that it can operate in either ideal or nonideal conditions; i.e., the accuracy of the estimation of the facial skin temperature by the thermal-based system is invariant to ambient illumination.

In this work, we studied an application of this technology for field temperature and heat stress identification under the rest, exertion, and rehabilitation aspects of first-responder operations.

For that purpose, we have employed a middle-wave infrared imaging system that has the highest thermal sensitivity in the market. Experimental results indi-

cate that this technology is capable of predicting the core body temperature of human subjects at a distance. The camera was used to monitor the faces of participants performing simulated field operations while wearing wildland firefighter protective garments. The main benefit of performing such a study is to assist in understanding the level of efficiency that thermal imaging-based monitoring systems have in detecting exertional heat stress.

## METHODS

### Ethics Approval

This study was approved by the University of Pittsburgh Institutional Review Board. Written informed consent was obtained from all subjects prior to any intervention.

### Participants

Six healthy men volunteered to participate. These subjects were a convenience sample from a larger study comparing ingestion of ice slurry vs. temperate water before exercise. Results of the larger study are reported separately. In this report, all subjects were precooled prior to exertion and were followed during exertion and recovery. The subjects were in good health, 18 years of age or older, and free of diagnosed cardiovascular, metabolic, and respiratory disease.

### Visit 1: Assessment of Cardiopulmonary Fitness

A study physician determined subject eligibility using medical history, physical examination, resting vital signs, and a 12-lead electrocardiogram (ECG). The subjects were asked to refrain from consuming caffeine, nicotine, and alcohol and from exercising 12 hours before the screening. Nude body mass was measured, to the nearest 0.005 kg, using a floor weighing scale (Kern ITB Version 2.0, Balingen, Germany). Skinfold thickness was measured at three sites (chest, abdomen, and thigh) in duplicate with a skinfold caliper (Beta Technology Inc., Cambridge, MD). The mean values were used to calculate skinfolds and estimate percentage body fat as previously described.<sup>9</sup>

Subjects performed a graded exercise Bruce treadmill test with open-circuit spirometry (Parvomedics Inc., Sandy, UT) to measure maximal oxygen consumption. Oxygen and carbon dioxide analyzers were calibrated prior to each test using standard referencing gases. A 12-lead ECG was obtained every 3 minutes during and after exercise. A cardiologist interpreted the test results to identify undiagnosed ischemic response to exercise.

## Visit 2: Assessment of Core Body Temperature during Precooling, Exertion, and Recovery in Wildland Firefighter Protective Garments

### Instrumentation

Core temperature ( $T_c$ ) was measured with an ingestible capsule and radio receiver (CoreTemp, HQ Inc., Palmetto, FL). Subjects ingested the capsule 8–12 hours before the protocol to avoid the effect of food or drink in the gastrointestinal tract.<sup>10</sup> Upon arrival to the laboratory, urine specific gravity (USG) was assessed with a handheld refractometer (SUR-NE, Atago U.S.A., Bellevue, WA) to ensure euhydration ( $USG \leq 1.020$ ) prior to beginning the protocol.

A heart rate (HR) monitor (Model T31, Polar Electro Oy, Kempele, Finland) was applied along with four reusable surface thermistors (Physitemp Instruments, Inc., SST-1 Skin Sensors, Clifton, NJ) placed on the left pectoralis major, infraspinatus, and the midpoint of the triceps brachii and quadriceps femoris muscles. Mean skin temperature ( $T_{sk}$ ) was calculated using the following formula:  $T_{sk} = \text{chest (0.25)} + \text{back (0.25)} + \text{thigh (0.3)} + \text{arm (0.2)}$  (1).<sup>11</sup> A fifth surface thermistor was placed over the left carotid artery identified by palpation midway between the clavicle and the angle of the mandible.

### Protocol

All subjects in this report completed the exercise trial after consuming ice slurry ( $0.1^\circ\text{C}$ ) with added syrup used for flavor, creating a 3% carbohydrate beverage. The ice slurries were made with a commercially available frozen drink machine (Ninja MasterPrep model QB900 30, Ninja, Boston, MA). During precooling, the subjects sat in wildland firefighting garments (Lion Apparel, Dayton, OH) while consuming  $1.25 \text{ g} \cdot \text{kg}^{-1}$  of drink every 5 minutes to ensure a standardized ingestion rate, totaling  $7.5 \text{ g} \cdot \text{kg}^{-1}$  over 30 minutes.

The subjects commenced the treadmill protocol approximately 5 minutes after finishing the drink ingestion. The subjects wore the wildland firefighting garments, a helmet, and a 20.4-kg backpack during exercise. The participants walked on a treadmill (Desmo, Woodway USA, Inc., Waukesha, WI) for 45 minutes at 4.0 mph in a heated enclosure ( $38.8^\circ\text{C} \pm 1.0^\circ\text{C}$ ,  $19.2\% \pm 2.2\%$  relative humidity). This protocol mimics the U.S. Forest Service Pack Test required of wildland firefighters.<sup>12</sup> The subjects were encouraged to maintain this pace, but whenever necessary they decreased the speed to a level that allowed them to complete the full protocol time interval. Each subject exercised for 45 minutes, in total, unless any one of the following conditions was met: 1) core temperature  $\geq 39.5^\circ\text{C}$ ; 2)

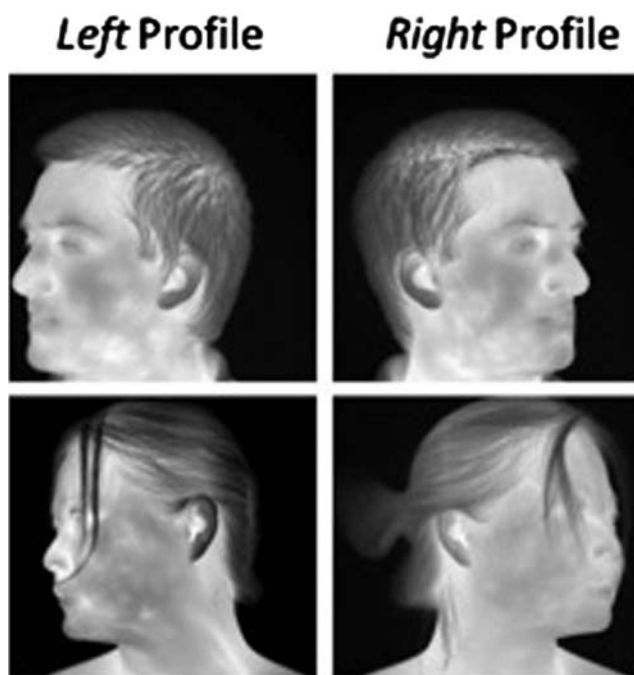


FIGURE 1. Sample profile facial images illustrating that subcutaneous information on different subjects varies, and that thermal facial images are capable of providing significant information about the temperature of the human body. Note that originally the camera acquires video frames where each pixel has a temperature value ranging from  $\sim 24^\circ\text{C}$  to  $41^\circ\text{C}$ . Then these frames are converted to grayscale images for display purposes.

HR greater than  $10 \text{ beats} \cdot \text{min}^{-1}$  over age-predicted maximum ( $220 - \text{age}$ ); 3) unsteady gait, making it unsafe to continue walking; or 4) subject request.

### Thermal Imaging Camera

The thermal camera used in this study was a high-definition middle-wave infrared camera (FLIR Systems, Inc., Wilsonville, OR). It is capable of acquiring thermal imprints of human skin and analyzing the thermal distributions and temporal variations (Fig. 1). The camera generates high-definition thermal images and can operate in diverse testing environments. It features a high-resolution  $1,024 \times 1,024$  (i.e., the spatial resolution of the system at any standoff distance) indium antimonide (InSb) focal plane array achieving high megapixel image resolution in a single thermal image. The effective focal length of the camera used is 50 mm. The detector used has  $1,024 \times 1,024$  pixels, with a pixel pitch of  $18 \mu\text{m}$ . The standoff distance used was approximately 1.5 m, where the target (human face) dimensions are approximately  $0.152 \times 0.229 \text{ m}$ . In terms of the output of the camera, the horizontal and vertical fields of view are the same (i.e.,  $0.365 \text{ rad}$ ) and the spot size ( $1 \text{ p} \times 1 \text{ p}$ ) is  $0.00054 \text{ m}^2$ . The spectral range of the camera is  $3\text{--}5 \mu\text{m}$ . The camera has a 14-bit dynamic

range, and a noise-equivalent temperature difference of less than 25 mK. The camera was outfitted with a 50-mm middle-wave infrared lens also provided from FLIR Systems.

The thermal sensitivity for an infrared camera is measured in millikelvins (mK). Thermal sensitivity of the camera is important and directly correlates with image quality. Current cameras are able to detect temperature differences as small as 0.03°C. This equates to a thermal sensitivity of 30 mK. Greater sensitivity of the camera leads to higher quality and more accurate images. The thermal camera that was used in the study has the highest sensitivity currently available in commercial thermal cameras.

The associated camera software (provided by FLIR Systems) was used not only to perform data collection, but also to perform regular calibration (before acquiring each set of thermal full frontal face images). Calibration ensures that the camera operates at its optimum performance and guarantees measurement accuracy and reliability. The software tool provided by FLIR Systems also performs nonuniformity correction, linearity correction, and bad pixel replacement (less than 0.5% of the pixels are bad/dead) as postprocessing operations on the imagery. The software was set to control the temperature scale limits (e.g., setting the temperature range from 28°C to 40°C that is the typical range of human body temperature) during data collection.

### Data Collection and Analysis

The standoff (camera-to-face) distance was set to 1.5 meters. Data were collected over a time period of 30 days. In the beginning of the session, the subjects were briefed about the data-collection process, after which they signed a consent document. The six subjects participating in this study resulted in a database containing 31 thermal and 31 visible videos of human faces for each subject, resulting in a total of 366 videos (~100 GB of data). The visible light camera (Canon 5D EOS Mark II, Canon U.S.A., Lake Success, NY) was used to illustrate the facial appearance of each subject during each phase of the protocol. Figure 2 illustrates the facial images of one of the participants acquired by the visible and the thermal cameras at four selected frames, representing the four different steps of the monitoring process of our study.

To establish a baseline for our study, the facial area of each subject was recorded by both the visible and the thermal cameras while the subject was relaxing on a chair. Then, during the “precooling step” every 5 minutes, the subject’s face was recorded while he was sitting on a chair ingesting ice slurry for 3 minutes in total by both cameras. This process was repeated seven times, resulting in two sets of visible- and

thermal-based videos of the human face of each subject (i.e., 35 minutes of video in total per subject per camera). During the subsequent exercise period, the subjects were asked to walk on a treadmill that was placed in a heated room while again being recorded by the two cameras. Exercise duration was 45 minutes, during which the subjects were recorded every 5 minutes (10 times in total). Finally, during the “recovery step,” the subjects’ faces were recorded every 5 minutes, i.e., 13 times in total. Sample facial images acquired at both the visible and thermal bands at one instance of each of the four aforementioned steps of the recording process (baseline, precooling, exercise, and recovery) are illustrated in Figure 2.

The proposed method for the estimation of the core body temperature using thermal imaging is contact-free; hence, in the absence of good tracking, even the slightest movement of the subject being recorded by the camera will shift the region of interest (subject’s face) from its initial selection. Although tracking methods could have been used to compensate for motion, they were not used in this study. The main reason was to manually select a sequence of good-quality frames to perform the measurements and prove our concept, avoiding any noisy measurements due to a potential inefficiency of the tracking algorithm. Thus, we performed an estimation of the maximum facial skin temperature over a number of frames, first by performing a manual selection of the region of interest, and then by manual tracking the subjects’ faces (frame by frame). For every recording (30 frames per second) that we obtained using the camera during rest and exercise, we monitored only the first 50 frames, i.e., <2 seconds (frames of nonfrontal faces were disregarded to exclude noisy estimations from our measurements). Each recording with the camera was synchronized with the temperature estimation using the other sensors (e.g., skin). Manual tracking was also helpful because, during exertion, most of the subjects were constantly moving and, thus, a sequence of good-quality full frontal facial images (frames) was not possible to be recorded. In such cases, it is very difficult to find areas of the face that allow a confident estimate of the maximum temperature in the facial region (such as the periocular region). Hence, the manual selection of the region of interest had to be arbitrary (usually an oval or a rectangular region was selected), and the region of interest was always (for all frames used to estimate the temperature) selected to be small enough to fit within the facial region of the subject being recorded.

Figure 3 outlines the salient stages used to passively estimate core body temperature with thermal imaging. For each frame (1,024 × 1,024 pixels), we first selected a region of interest within the subject’s face (a variable area, and thus a variable number of pixels). Within each region of interest, we estimated the maximum





FIGURE 2. Sample data collection. Note the region of interest in the thermal faces where the maximum temperature of the subject was measured. Also shown is the timeline for each step during which the measurement was acquired.

temperature over the first 50 frames of each recording (as described above). The median of the maximum temperatures was then calculated over 50 frames. This measure was used as an estimate of the core body temperature for each recording. Finally, these thermal imaging-based temperature measurements (estimates of core temperature) were compared with the core body temperature measured using the capsule, as well as the facial and skin temperatures using the skin sensors.

Note that, although the standoff distance was fixed to be 1.5 meters, the region of interest (selected area within each subject's face) varied (depending on the subject's facial structure and movement towards and away from the camera). We estimated the average number of pixels used for the calculation of the maximum temperature to be about ~160,000 pixels (i.e.,  $400 \times 400$  pixels, if the region of interest is selected to be rectangular).

## Statistical Analysis

We analyzed the data acquired at each step (epoch) of the monitoring process, i.e., precooling, exercise, and recovery. Within each epoch, we measured the 1) core body temperature, 2) skin temperature over the carotid artery, 3) mean skin temperature, and 4) facial skin temperature, estimated using thermal imaging. Then, we computed the correlations between thermal imaging-estimated temperature and the conventional core and skin temperature measurements. Bland-Altman plots were also generated to test the agreement of temperatures during exertion.

## RESULTS

### Participant Characteristics

The subjects were fit men (Table 1). Five subjects completed the entire 45-minute bout of exercise, whereas

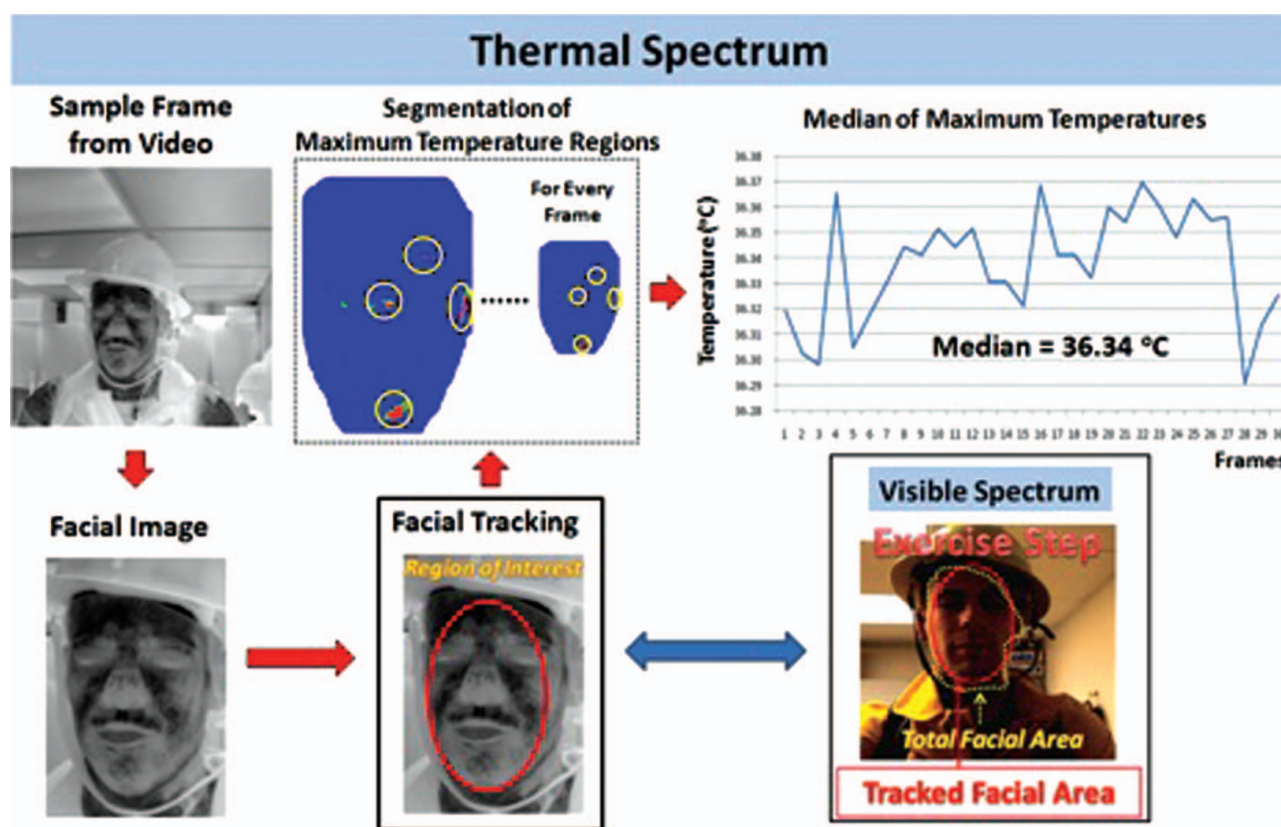


FIGURE 3. Illustration of the process of computing the median of the maximum temperatures over one (out of the 31 total) video recording using the thermal camera.

one subject reached volitional fatigue after 30.5 minutes, resulting in an average ( $\pm$  standard deviation) exercise duration of 42.6 ( $\pm 5.9$ ) minutes and walking distance of 4.2 ( $\pm 0.6$ ) km. At the end of exercise, the mean HR was 152 ( $\pm 33$ ) bpm and the mean core body temperature was 38.3°C ( $\pm 0.7$ °C).

## Thermal Measurements

A visual relationship between core temperature and thermal imaging of the face could be identified in all subjects, with the closest relationship and best agreement occurring during exercise (Fig. 4). Correlations were identified for thermal imaging and all measured temperatures with the exception of core body temperature during precooling (Table 2). However, a negative correlation between thermal imaging temperature and mean skin temperature was identified during precooling and recovery.

TABLE 1. Subject Characteristics

Age (yr)	Height (cm)	Mass (kg)	VO <sub>2max</sub> (mL/kg/min)	Body Fat (%)
34.5 $\pm$ 9.1	181.9 $\pm$ 5.8	89.7 $\pm$ 17.7	50.4 $\pm$ 8.8	14.6 $\pm$ 6.7

Values are expressed as mean  $\pm$  standard deviation.

VO<sub>2max</sub> = maximum volume of oxygen consumption.

The Bland-Altman test of agreement during exercise revealed that the majority of measurement pairs were within two standard deviations of the measured temperature (Fig. 5). The bias between core body temperature and thermal imaging of the face was  $-0.07$ °C (1.4°C). The biases from the temperature sensor placed on the skin over the carotid artery ( $-1.9$ °C [1.5°C]) and body mean skin temperature ( $-1.3$ °C [1.4°C]) were both larger than the bias with core body temperature during exercise.

## DISCUSSION

High-resolution thermal imaging of the facial features during exertion in wildland firefighting garments captured measures of temperature that were highly correlated and in close agreement with core body temperature. While the bias of the agreement was greater during precooling and recovery, correlations remained high during these intervals, indicating that it is possible to identify a correction factor to estimate core body temperature during periods of nonexertion. Potential applications for this technology include screening first responders (e.g., firefighters and hazardous materials technicians) for heat stress and deployment to monitor participants at mass-gathering athletic events such as marathons or ultra-endurance races.

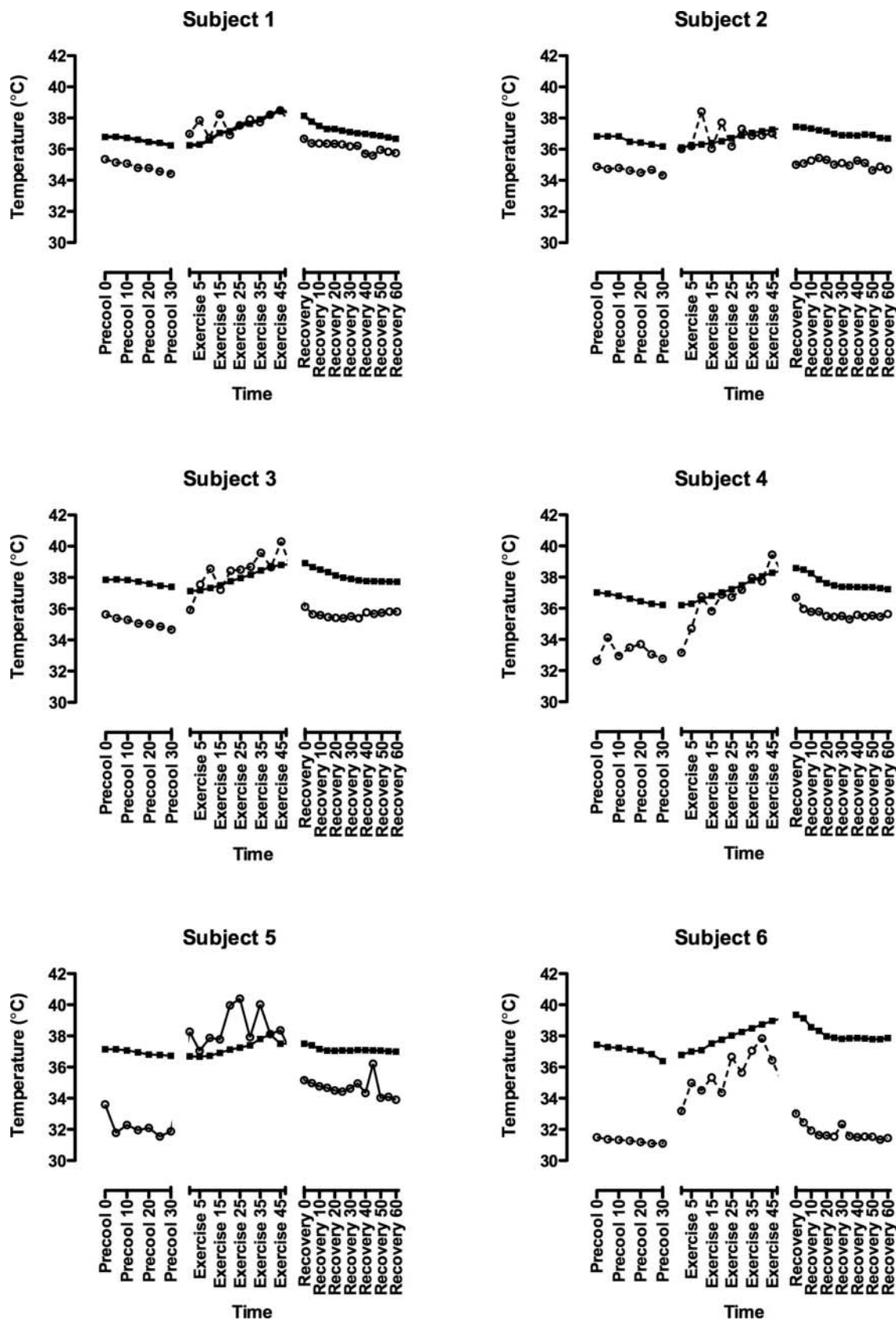


FIGURE 4. Body core temperature (squares) and thermal imaging temperature (open circles) of the face measured during precooling, exercise, and recovery in the six subjects.



TABLE 2. Correlations between Thermal Imaging Temperature and Other Measured Temperatures

	Precooling			Exercise			Recovery		
r	Core	Carotid	Mean Skin	Core	Carotid	Mean Skin	Core	Carotid	Mean Skin
p-value	0.086	0.560	-0.421	0.411	0.527	0.473	-0.253	0.575	-0.342
	0.590	< 0.001	0.006	0.001	< 0.001	< 0.001	0.026	< 0.001	0.002

It is not clear why the amount of bias differs between exertion and resting phases. The protocol required the subject to work in a heated room while wearing protective clothing, so the higher ambient temperature may have contributed to these differences. However, the

temperature across the face was not uniform. The areas displaying the maximum temperature were measured and typically corresponded with the course of the facial artery. Given the higher HR during exertion and activation of the thermoregulatory mechanisms, it is likely that these areas were well perfused with blood, during which the temperature more closely approximated core body temperature than might be observed during rest. Future iterations of the technology may need to consider HR and ambient temperatures when estimating core body temperature.

Correlations between core body temperature and thermal imaging temperature were inconsistent over the course of the study. Although a positive correlation was seen during exertion, a negative correlation was seen during recovery and no correlation could be identified during precooling. This lack of a relationship during precooling may be due to local cooling of the facial structures from the ice slurry. The inverse relationship seen in the recovery phase appears to be the product of a static thermal imaging temperature over the recovery period and a falling core temperature. However, the correlation between thermal imaging temperature and skin temperature over the carotid artery was always positive and significant. This might be expected given that the facial artery is a branch of the external carotid artery. However, the agreement between the thermal imaging of the face and the skin over the carotid artery was worse than the agreement with core body temperature. We hypothesized that this may be due to the thickness of the skin and physiologic structures overlying the carotid artery. Furthermore, variation in body habitus among individuals may limit the utility of the neck as a measurement site.

Previous work using thermal imagers to estimate core body temperature have largely examined the ability to detect fever. A study of 310 individuals reporting to the emergency department during the severe acute respiratory syndrome (SARS) epidemic found that measuring temperature with thermal imagers in the area of the medial canthus provided the best estimate of the temperature measure with a tympanic thermometer.<sup>13</sup> In that study, it was determined that a thermal imager could be set to signal an alarm when measured temperature exceeded 36.3°C, to identify individuals requiring additional screening. A follow-up study of 86 febrile and 410 normothermic patients reported a sensitivity of 90.7% and a specificity of 75.8% to detect a fever, defined as

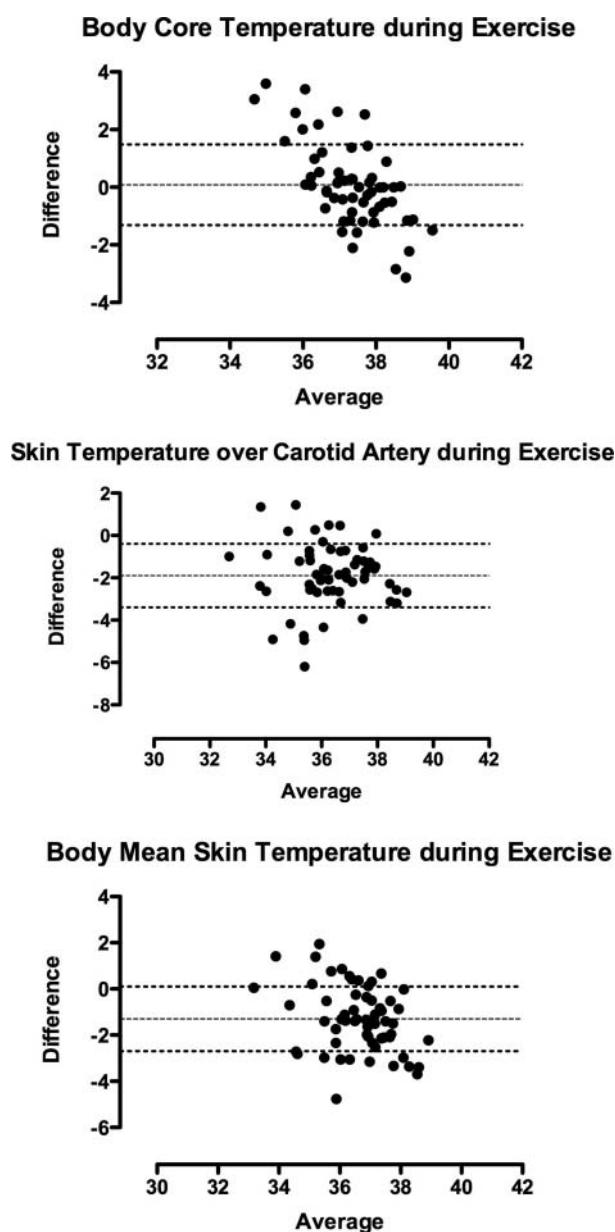


FIGURE 5. Bland-Altman tests of agreement between thermal imaging temperature of the face and body core temperature (top panel), skin temperature over the carotid artery (middle panel), and body mean skin temperature (bottom panel).



body temperature  $>37.7^{\circ}\text{C}$ .<sup>14</sup> More recently, a study employing three different thermal imaging cameras reported sensitivity of 91% and 90% and specificity of 86% and 80% to detect fever in the emergency department via the two best performing cameras.<sup>15</sup>

The present report expands upon previous work by examining the utility of a high-resolution thermal imaging camera to estimate core body temperature during rest and exertion. We are aware of only one other study using similar technology to estimate temperature during exertion.<sup>16</sup> That study contrasts with the present findings in that the rise of core body temperature during exercise was not detected by the thermal imaging device. However, that study deployed a near-infrared camera with an extended range (0.8–2.5  $\mu\text{m}$ ) and lower-resolution (320  $\times$  256) input. In the present report, the thermal imager featured a high-resolution 1,024  $\times$  1,024 InSb focal plane array achieving megapixel image resolution in a single thermal image. The high-resolution input and high thermal sensitivity of the camera allowed for more precise measurements. The study by Teunissen and Daanen (2011) reported difficulty with imaging the medial canthus in all subjects and all conditions.<sup>16</sup> The advantage of our methodology is that it is capable of scanning the entire face of the subject under study for maximum temperatures, providing greater flexibility in obtaining an accurate estimate of temperature.

Near-term applications for this technology could include screening multiple subjects in short periods of time to identify those with suspected hyperthermia, such as during sporting events, responders entering emergency incident rehabilitation, and military patrols. After correction factors have been identified for nonexertion conditions, the technology could be used to identify those emergency responders and workers who are too hyperthermic to return to work. It can also be used for screening large numbers of subjects for fever at ports of entry and public areas during periods of pandemics or the release of biologic agents.

## LIMITATIONS AND FUTURE RESEARCH

The principal limitation of this study is the small number of subjects who were available for analysis. In spite of this, strong correlations and agreement during exertion encourage additional studies in this area. These data are further strengthened by employing rigorous data-collection methods and direct measurement of core body temperature, instead of surrogates (e.g., tympanic and oral thermometry) that may be difficult to accurately use during or following exertional heat stress.<sup>5</sup> Additionally, we do not have data for passive heating or febrile conditions, representing additional areas of exploration. Data collection was performed in a controlled indoor environment, where

the room temperature and illumination were stable and placed away from the subject. Outdoor conditions or nearby heat/light sources may confound the operation.

## CONCLUSIONS

High-resolution thermal imaging in the middle-wave infrared spectrum (3–5  $\mu\text{m}$ ) can be used to accurately estimate core body temperature during exertion in a hot room while participants are wearing wildland firefighting thermal protective clothing. Although this technology is promising, it must be refined. Using alternative measurement sites such as the skin over the carotid artery, using multiple measurement sites, or adding pulse detection is expected to improve the estimation of body temperature by thermal imagery.

## References

1. Lieberman HR, Bathalon GP, Falco CM, Kramer FM, Morgan CA 3rd, Niro P. Severe decrements in cognition function and mood induced by sleep loss, heat, dehydration, and undernutrition during simulated combat. *Biol Psychiatry*. 2005;57:422-9.
2. Horn GP, Gutzmer S, Fahs CA, et al. Physiological recovery from firefighting activities in rehabilitation and beyond. *Prehosp Emerg Care*. 2011;15:214-25.
3. Hostler D, Reis SE, Bednez JC, Kerin S, Suyama J. Comparison of active cooling devices with passive cooling for rehabilitation of firefighters performing exercise in thermal protective clothing: a report from the Fireground Rehab Evaluation (FIRE) trial. *Prehosp Emerg Care*. 2010;14:300-9.
4. Colburn D, Suyama J, Reis SE, et al. A comparison of cooling techniques in firefighters after a live burn evolution. *Prehosp Emerg Care*. 2011;15:226-32.
5. Pryor RR, Seitz JR, Morley J, et al. Estimating core temperature with external devices after exertional heat stress in thermal protective clothing. *Prehosp Emerg Care*. 2012;16:136-41.
6. Ganio MS, Brown CM, Casa DJ, et al. Validity and reliability of devices that assess body temperature during indoor exercise in the heat. *J Athl Train*. 2009;44:124-35.
7. Bourlail T, Buddharaju P, Pavlidis I, Bass B. On enhancing cardiac pulse measurements through thermal imaging. Presented at: International Conference on Information Technology and Applications in Biomedicine, Larnaka, Cyprus, November 2009.
8. Bourlail T, Buddharaju P, Pavlidis I, Bass B. Methodological advances on pulse measurement through functional imaging. In: Garbey M, Bass BL, Collet C, de Mathelin M, Tran-Son-Tay R (eds). *Computational Surgery and Dual Training, Advances in Pattern Recognition*. New York: Springer, 2010, pp 101-21.
9. Jackson AS, Pollock ML. Prediction accuracy of body density, lean body weight, and total body volume equations. *Med Sci Sports*. 1977;9:197-201.
10. Wilkinson DM, Carter JM, Richmond VL, Blacker SD, Rayson MP. The effect of cool water ingestion on gastrointestinal pill temperature. *Med Sci Sports Exerc*. 2008;40:523-8.
11. Ayling JH. Regional rates of sweat evaporation during leg and arm cycling. *Br J Sports Med*. 1986;20:35-7.
12. Sharkey B. Development and validation of a job related work capacity test for wildland firefighters. Presented at: International Association of Wildland Fire Safety Summit, Sydney,

- Australia, 1999. Available at: <http://www.iawfonline.org/proceedings.php>. Accessed October 19, 2011.
13. Ng EY, Kaw GJ, Chang WM. Analysis of IR thermal imager for mass blind fever screening. *Microvasc Res*. 2004;68:104-9.
  14. Ng EY. Is thermal scanner losing its bite in mass screening of fever due to SARS? *Med Phys*. 2005;32:93-7.
  15. Nguyen AV, Cohen NJ, Lipman H, et al. Comparison of 3 infrared thermal detection systems and self-report for mass fever screening. *Emerg Infect Dis*. 2010;16:1710-7.
  16. Teunissen LP, Daanen HA. Infrared thermal imaging of the inner canthus of the eye as an estimator of body core temperature. *J Med Eng Technol*. 2011;35:134-8.